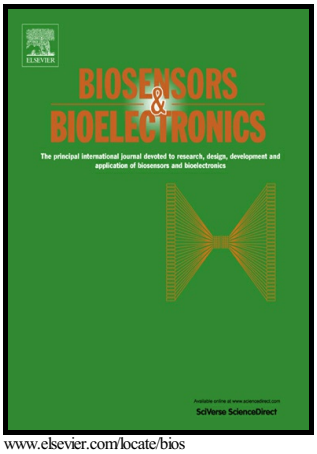

www.elsevier.com/locate/bios

Enhancing surface functionality of reduced graphene oxide biosensors by oxygen plasma treatment for Alzheimer's disease diagnosis

Myung-Sic Chae, Jinsik Kim, Dahye Jeong, YoungSoo Kim, Jee Hoon Roh, Sung Min Lee, Youhee Heo, Ji Yoon Kang, Jeong Hoon Lee, Dae Sung Yoon, Tae Geun Kim, Suk Tai Chang, Kyo Seon Hwang

PII: S0956-5663(16)31067-3
DOI: http://dx.doi.org/10.1016/j.bios.2016.10.049
Reference: BIOS9271

To appear in: *Biosensors and Bioelectronic*

Received date: 25 August 2016
Revised date: 5 October 2016
Accepted date: 19 October 2016

Cite this article as: Myung-Sic Chae, Jinsik Kim, Dahye Jeong, YoungSoo Kim Jee Hoon Roh, Sung Min Lee, Youhee Heo, Ji Yoon Kang, Jeong Hoon Lee, Dae Sung Yoon, Tae Geun Kim, Suk Tai Chang and Kyo Seon Hwang, Enhancing surface functionality of reduced graphene oxide biosensors by oxyge plasma treatment for Alzheimer's disease diagnosis, *Biosensors an Bioelectronic,* http://dx.doi.org/10.1016/j.bios.2016.10.049

Enhancing surface functionality of reduced graphene oxide biosensors by oxygen plasma treatment for Alzheimer's disease diagnosis

Myung-Sic Chae [a,b,†], Jinsik Kim [a,†], Dahye Jeong [a], YoungSoo Kim [c,d], Jee Hoon Roh [e], Sung Min Lee [f], Youhee Heo [a], Ji Yoon Kang [a], Jeong Hoon Lee [g], Dae Sung Yoon [h], Tae Geun Kim [b*], Suk Tai Chang[f,**], Kyo Seon Hwang [a,***]

[a]Center for BioMicrosystems, Korea Institute of Science and Technology (KIST), Seoul 02792, Republic of Korea

[b]School of Electrical Engineering, Korea University, Seoul 02841, Republic of Korea

[c]Convergence Center for Dementia, Korea Institute of Science and Technology (KIST), Seoul 02792, Republic of Korea

[d]Department of Pharmaceutical Science, College of Pharmacy, Kyung Hee University, Seoul 02447, Republic of Korea

[e]Department of Neurology, Asan Medical Center, Ulsan University College of Medicine, Seoul 05505, Republic of Korea

[f]School of Chemical Engineering and Materials Science, Chung-Ang University, Seoul 06974, Republic of Korea

[g]Department of Electrical Engineering, Kwangwoon University, Seoul 01897, Republic of Korea

[h]School of Biomedical Engineering, Korea University, Seoul 02841, Republic of Korea

tgkim1@korea.ac.k

stchang@cau.ac.kr

kshwang@kist.re.kr

*Corresponding author. Tel: +82-2-3290-3255, Fax: +82-2-921-0544.

**Corresponding Author. Tel: +82-2-820-5889, Fax: +82-2-824-3495.

***Corresponding Author. Tel: +82-2-958-6727, Fax: +82-2-958-6910.

ABSTRACT

We performed oxygen plasma treatment on reduced graphene oxide (rGO) to improve its surface reactivity with respect to biomolecular interactions. Oxygen-plasma-treated rGO surfaces were employed as reactive interfaces for the detection of amyloid-beta (Aβ) peptides, the pathological hallmarks of Alzheimer's disease (AD), as the target analytes. By measuring the changes in electrical characteristics and confirmation through topographic analysis, the oxygen-plasma-treated rGO sensors had enhanced surface functionality for better antibody immobilization and sensing performance, with a 3.33-fold steeper slope for the electrical responses versus analyte concentration curve (logarithmic scale) compared to the untreated. The elicited biomolecular reactivity of the rGO surfaces with the oxygen plasma treatment remained at 46–51% of the initial value even after aging for 6 h in ambient conditions. This phenomenon was also confirmed by pretreating the rGO surfaces with a blocking agent and subsequently subjecting them to antibody immobilization. Finally, the feasibility of the oxygen-plasma-treated rGO sensors as a diagnostic tool was evaluated with clinical samples of neural-derived exosomal Aβ peptides extracted from apparent AD patients and normal controls (NC). In contrast to the untreated sensors ($p = 0.0460$), the oxygen-plasma-treated rGO sensors showed a significant p-value in the identification of clinical samples of AD and NC subjects ($p < 0.001$). These results suggest that oxygen plasma treatment improves sensor performance without complicated fabrication procedures and should aid in the development of novel diagnostic tools based on carbon nanomaterials.

KEYWORDS: Reduced graphene oxide, oxygen plasma treatment, biosensor, Alzheimer's diseases, exosome

1. Introduction

For the past few decades, carbon nanomaterials have been employed widely as biological and chemical interfaces for molecular detection. Graphene, a two-dimensional hexagonal network of carbon atoms, has attracted the most interest among the various carbon materials available since its discovery in 2004. Owing to the remarkable electrical properties and ease of surface modification and functionalization of graphene, it has been explored widely for developing electrical biosensors (Balasubramanian and Kern, 2014; Ohno et al., 2010; Schedin et al., 2007). The use of reduced graphene oxide (rGO) has allowed for graphene-based biosensors to find wide applicability, owing to the numerous advantages of rGO, which includes its simple synthesis, large accessible surface area, and good biocompatibility. Several studies have reported that biomolecular interactions on the rGO surface can affect its inherent properties, and its charge may lead to geometric deformations or surface-charge effects (Balasubramanian and Kern, 2014; Kochmann et al., 2012). Consequently, biological interactions with different kinds of biomolecules such as DNA (Lu et al., 2009) and proteins (D.-J. Kim et al., 2013) as well as living bacteria (Hernández et al., 2014) may cause changes in the electrical characteristics of rGO.

Of the various approaches that can be used for the surface modification of rGO-based devices, plasma-assisted surface treatment is a commonly used one. This technique is used widely with various polymers and carbon nanomaterials to modify their surface properties, for selectively etching the surfaces of such materials, and for removing any residual photoresist (Childres et al., 2011; Chirila et al., 2005; Mao et al., 2009). In particular, the use of an oxygen plasma allows the biocompatibility of a material to be modified while ensuring that

its bulk properties remain unchanged (Balazs et al., 2003; J.-Y. Lee et al., 2009). Yang et al. (Xue and Yang, 2007) reported the chemical modification of self-assembled monolayers of octadecyltrichlorosilane using an oxygen plasma treatment. This increased the density of the surface functional groups, thus resulting in greater surface functionalization and enhanced biomolecular recognition.

In this study, we investigated the effects of the oxygen plasma treatment of rGO-based biosensors to enhance their sensing performance in biomolecular detection and to develop a clinical platform that would be applicable in AD diagnosis without the need for complex modification techniques (Y.-K. Kim et al., 2011; Jang et al., 2015) or a labeling process. As depicted in **Fig. 1**, the biological reactivity of the plasma-treated rGO sensors was compared with that of an untreated rGO sensor in the detection of target analytes, namely, amyloid-beta (Aβ) peptides. By measuring the change in the resistance of the sensors before and after interactions with the target analytes, the enhancement in the biological reactivity of the rGO surfaces could be evaluated. To begin with, we prepared rGO thin films on wafer-level SiO_2 insulating substrates using a simple and cost-effective deposition method; these films were used as the biological sensing interfaces. Then, an oxygen plasma treatment was performed on the rGO surfaces to modify their functionality. By controlling the radiofrequency (RF) power of the plasma and the duration of exposure, the optimal conditions for the oxygen plasma treatment of the rGO surfaces could be established without generating defects or causing the undesired etching of the rGO films. This was confirmed based on the changes in the thickness profiles of the rGO films as well as through electrical and chemical analyses. The oxygen plasma treatment of the rGO surfaces aided the covalent immobilization of antibody molecules on them. This could be visualized through topographic analyses performed using atomic force microscopy (AFM).

The changes in the electrical characteristics of the antibody-immobilized oxygen-plasma-treated rGO sensors in response to target-specific recognition interactions were greater than those of the untreated sensor. It was also found that the improvement in the surface functionality of rGO with the oxygen plasma treatment diminished with aging. This phenomenon was also confirmed by subjecting the rGO sensors to a pretreatment with 5 M ethanolamine (ETA) as a blocking agent and then evaluating the biological reactivity of the sensors. Finally, the oxygen-plasma-treated rGO sensors were successfully used to distinguish between plasma samples collected from Alzheimer's disease (AD) patients and those from normal control (NC) subjects based on the detection of Aβ peptides in the extracellular vesicles of neuronal cells.

2. Experimental

2.1 Deposition of rGO thin films and fabrication of rGO sensors

The rGO thin films were prepared through a two-step process: deposition of GO and reduction of GO. A schematic illustration of the overall fabrication process is shown in **Fig. 2A-D**. As was the case in our previous studies, the GO flakes were produced by the modified Hummers method and exfoliated under ultrasonication. The GO flakes were then dispersed using an ultracentrifuge and mixed with ultrapure Milli-Q water to obtain a GO solution with a concentration of 2.6 mg mL^{-1} (N. H. Kim et al., 2012). Next, GO films were formed by the meniscus-dragging deposition (MDD) technique on 4-inch SiO_2 substrates **(Fig. 2A)**. In order to deposit the GO thin films, a glass plate (127 × 127 mm^2) was used after being cleaned with a piranha solution (H_2SO_4/H_2O_2= 3:1). The GO solution (100 μL) was dropped between the SiO_2/Si substrate and the deposition plate, which was placed at a contact angle of 30 with respect to the substrate. A motorized stage (AL1-1515-3S, Micro Motion Technology)

allowed the deposition plate to be moved in order to spread the GO solution on the substrate at a constant speed of 20 mm s^{-1}; this was done 20 times. After the GO thin films had been deposited, they were chemically reduced with hydriodic acid (HI) vapor at 80 °C for 3 h, resulting in the formation of rGO thin films. These rGO thin films were employed as biological sensing interfaces and were used to fabricate individual electrical devices using microelectromechanical systems (MEMS) techniques **(Fig. 2B)** (J. Kim et al., 2016). A photoresist (AZ GXR-601, AZ Electronic Materials) was spin-coated and developed to form etch masks. The photoresist-patterned rGO thin films were then fully etched in a reactive-ion etcher with an RF power of 300 W for 30 s in an O_2 atmosphere. After the patterning of the rGO films, the lift-off process and photolithography were used to form gold electrodes to act as source-drain contacts **(FIg. 2C)**. A gold layer (200 nm) was deposited with a Cr adhesive layer (50 nm) using an electron-beam evaporator. The substrate was cleaned with acetone, 2-propanol, and methanol between each step. Next, the oxygen plasma treatments were performed using a microwave plasma asher (PP41, Plasma Finish) at output powers of 25, 50, and 100 W for 10, 20, and 30 s; the flow rate was 100 sccm **(Fig. 2D)**. The individual rGO sensors had dimensions of 11.6 × 8.10 mm^2 and included 14 rGO patterns (**Fig. 2E**), with each rGO pattern having the dimensions of 100 × 50 μm^2 and gold electrodes as the source-drain contacts **(Fig. 2F)**.

2.2 Measurement and characterization

The thickness profiles of the rGO thin films subjected to the oxygen plasma treatment under different conditions were measured by AFM (XE-100, Park Systems, Republic of Korea), while the electrical characteristics were measured using a probe station (AP-8000, Unitek Corp., Republic of Korea) with a semiconductor analyzer (B1500A, Agilent Technologies,

USA). The chemical properties of the oxygen-plasma-treated rGO patterns were measured by Raman spectroscopy (inVia Raman Microscope, Renishaw, UK). The height profiles for the topographic analyses of the antibody-immobilized rGO surfaces were obtained in the tapping mode of AFM (Multimode V, Veeco, USA) using a cantilever tip (TESP, Bruker, USA).

2.3 Surface functionalization

Prior to surface functionalization with an antibody, the rGO sensors were washed with 2 mL of acetone, 2-propanol, methanol, and distilled water to eliminate any organic contaminants and subsequently dried with pure nitrogen gas. Next, the rGO sensors were pre-incubated in 20 µL of a 1-ethyl-3-[3-dimethylaminopropyl]-carbodiimide (EDC, 2 mM, Sigma Aldrich, USA) and N-succinimide (NHS, 8 mM, Sigma Aldrich, USA) solution diluted in 10 mM phosphate buffered silane (PBS) for 1 h at room temperature. Then, the sensors were incubated for 2 h at room temperature in a mixed solution of EDC (2 mM), NHS (8 mM), and the 6E10 monoclonal antibody (Covance, USA, 10 µg mL^{-1}), in order to make the antibody molecules covalently bond on the rGO surfaces. ETA (10 mM, Sigma Aldrich, USA) was used to prevent undesired covalent bonding. The prostate-specific antigen (PSA) antibody (Fitzgerald, USA, 10 µg mL^{-1}) was also immobilized on the rGO sensors using the same procedures for use as a negative control.

2.4 Exosome isolation and exosomal Aβ protein preparation

A total of 30 samples were obtained from AD patients (N = 15) and NC subjects (N = 15). All 30 subjects underwent clinical interviews, neurological examinations, detailed neuropsychological and laboratory tests, and 3T-MRI scans at Asan Medical Center, Seoul,

Korea. The AD patients fulfilled the diagnostic criteria for probable AD proposed by the National Institute of Neurological and Communicative Disorders and Stroke and the Alzheimer's Disease and Related Disorders Association (McKhann et al., 1984). Further, the NC subjects fulfilled the following criteria: (1) no history of neurological or psychiatric disorders except for memory complaints; (2) normal cognition as measured by neuropsychological tests; (3) normal activities related to daily living; and (4) no structural lesions in the brain (Roh et al., 2011). The institutional review board of Asan Medical Center approved the study protocol and informed consent was obtained from each participant.

The neural exosomes were derived from plasma samples by the ExoQuick precipitation method using a centrifuge (Huang et al., 2013; Peterson et al., 2015). The plasma samples (150 µL) were mixed with a recalcification reagent (50 µL), which was a mixture of 90 mM NaCl and 40 mM $CaCl_2$. The recalcified plasma samples were then incubated with 5 µL of 2% thromboplastin-D (Fisher, USA) at room temperature. Next, the samples were centrifuged at 10,000 g for 5 min using a centrifuge (WiseSpin CF-10, Daehan Scientific, Republic of Korea) to remove the debris, and the supernatants were mixed thoroughly with 50 µL of ExoQuick precipitation solution (System Bioscience, Inc., Mountain View, USA). After being incubated at 4 °C, the resultant exosome suspensions were centrifuged at 1500 g for 30 m at 4 °C. Each pellet was resuspended in PBS containing protease inhibitors (cOmplete Mini, EDTA-free, Roche Applied Science, USA). To the diluted exosome samples (150 µL), 80 µL of 3% bovine serum albumin (BSA) was added, and the mixtures were incubated with the biotinylated mouse monoclonal antihuman GRIA2 antibody (MBS802121, MyBiosource, USA) for 1 h at 4 °C on a rotator. Next, 40 µL of 3% BSA and 20 µL of streptavidin-agarose resin (Thermo Fisher Scientific, USA) were added to the samples. After centrifugation at 250 g (MICRO 17TR, Hanil Science, Republic of Korea) for 10 min at 4 °C, the supernatants were removed, and 40 µL of glycin-HCl (50 mM, pH 3.0) was added to the pellets, which

were suspended using a vortex mixer for 10 s to detach the exosomes. The suspensions were centrifuged at 250 g (MICRO 17TR, Hanil Science, Republic of Korea) for 10 min at 4 °C, and the supernatants were removed. Finally, 4 μL of Tris-HCl (1 M, pH 8.6) was added for neutralization, and the pellets were resuspended in PBS (initial volume).

3. Results and discussion

3.1. Characterization of oxygen-plasma-treated rGO biosensors

In order to fabricate the rGO sensors through MEMS techniques, first, highly uniform rGO thin films were prepared on 4-inch SiO_2 substrates by the MDD technique and a subsequent chemical reduction process (N. H. Kim et al., 2012; Ko et al., 2014). Then, patterns were etched in the rGO films using a reactive-ion etcher, and Cr/Au pads to be used as contact electrodes were formed by the conventional lift-off technique. As our previous studies (J. Kim et al., 2016), the fabricated rGO sensors exhibited a sheet resistance of 9.32 $k\Omega\ sq^{-1}$ on average, with the chip-to-chip distribution being 2.3%. Next, the rGO sensors were treated with an oxygen plasma using a plasma asher, in order to enhance their surface functionality. The surface reactivity, which depended on the exposure conditions, was measured in the form of the relative changes in the electric resistance of the sensors using a semiconductor analyzer. In addition, the time-dependent characteristics of the rGO surfaces during biological interactions were also observed.

To begin with, the effects of the oxygen plasma treatment of the fabricated rGO sensors on their mechanical and electrical properties were investigated (**Fig. 3**). The thicknesses of the rGO patterns after the oxygen plasma treatment under different conditions were measured using AFM. The thickness decreased gradually by 2–3 nm from the initial value after the oxygen plasma treatment under mild conditions (RF power of 25 W; exposure time of 10–30

s and RF power of 50 W; exposure time of 10 s). However, the thickness decreased significantly for RF powers greater than 50 W even when the exposure time was 20 s. An RF power of 100 W and exposure time of 30 s completely removed the rGO thin film. Considering that the thickness of the untreated rGO thin films was 8–10 nm (N. H. Kim et al., 2012), it was concluded that an RF power of less than 50 W and an exposure time of 10 s were suitable for ensuring that the rGO patterns were etched without the films being removed. The change in the resistance, $(R_{oxy}-R_0)/R_0$, was measured and found to vary with the oxygen plasma treatment conditions; here, R_{oxy} is the resistance of the rGO patterns after plasma exposure under different conditions, and R_0 is the resistance of the untreated rGO patterns. The changes in the thickness profiles corresponding to the changes in the resistance are depicted by the red blocks in **Fig. 3**. The resistance increased significantly after exposure at RF powers greater than 50 W for 20 s. Thus, the resistance was strongly dependent on the thickness profile of the patterns after etching. On the other hand, the rGO patterns plasma-treated at RF powers lower than 50 W for 10 s exhibited an increase in resistance of only 3–5%. This suggested that the oxygen plasma treatment should be performed at an RF power lower than 50 W for 10 s, so that the mechanical and electrical properties of the native rGO films are not adversely affected.

A detailed comparison of the effects of the different conditions for the oxygen plasma treatment was performed through a chemical analysis. Raman spectroscopy was performed to characterize the rGO thin films exposed to the oxygen plasma under different conditions (**Fig. S1**). Scanning Raman spectroscopy yields insights into the nature and placement of defects on graphene surfaces and allows them to be visualized over large areas. Peaks attributable to the D band (~1350 cm^{-1}) and G band (~1590 cm^{-1}) appeared in the case of all the rGO thin films, regardless of the oxygen plasma treatment conditions. In principle, the ratio of the intensities of the D and G bands (I_D/I_G) is reflective of the defects, vacancies, or distortions

present in the sp2 domain of the rGO structure (Beams et al., 2015). In this study, it was observed that the I_D/I_G ratio increased slightly as the RF power for the oxygen plasma treatment was increased from 1.84 to 2.19, indicating that the damage caused to the films and the number of dislocations formed were insignificant. However, a small number of defects were introduced with the increase in the RF power. In contrast to previous studies on the plasma treatment of single-layered or few-layered pristine graphene thin films for improving their functionality (Nourbakhsh et al., 2010), in the present study, the oxygen plasma treatment of multilayered rGO thin films did not significantly affect their surface chemistry or lead to their oxidation. Instead, only their mechanical properties were affected, with the properties being dependent on the respective etching profiles.

3.2 Evaluation of biological functionality and sensing performance for the target-analyte detection

To evaluate the effects of the oxygen plasma treatment on the biomolecular sensing ability of the rGO sensors, Aβ peptides, one of the pathogenic hallmarks of AD, were used as the target analytes. Aβ peptides are small molecules consisting of only 36–43 amino acids and prone to cleavage with the formation of larger and insoluble plaques, such as neurotoxic oligomers or fibrils, that cause neuronal dysfunction and cell death, which are strongly associated with AD progression (Murphy and LeVine, 2010; O'Brien and Wong, 2011). Therefore, quantification of Aβ peptides may characterize disease state and can play a major role in clinical diagnosis of AD. Several efforts have been made to detect the synthetic target analytes with various biosensors at the laboratory stage; however, most clinical analyses with human-derived samples of AD were limited to conventional methods such as commercial enzyme-linked immunosorbent assay (ELISA) kits (Table S1). In this study, we tried to conduct target

analyte detection with both synthetic and clinically relevant samples by using the rGO-based biosensors compared to previous studies.

In order to detect the target molecules, the rGO sensors were functionalized with the specific antibody, and the target analytes were introduced on the sensors to allow for the specific binding interactions. The changes in the resistances of the oxygen-plasma-treated and untreated rGO sensors before and after these interactions were measured and compared. The monoclonal 6E10 antibody, which recognizes the first 1–16 amino acid residues of human Aβ peptides, was immobilized on the rGO surfaces through incubation with coupling agents.

Fig. 4A shows a comparison of the changes in the electric resistances and surface topologies of the untreated and oxygen-plasma-treated rGO sensors after antibody immobilization. The gray blocks in **FIg. 4A** represent the changes in the resistances, $(R_{ab} - R)/R$, of the oxygen-plasma-treated rGO and untreated rGO sensors; here, R_{ab} is the resistance of the rGO sensors after antibody immobilization and R is the initial resistance of the rGO sensors before surface functionalization. The oxygen-plasma-treated rGO sensors showed a 13.9% increase in resistance after antibody immobilization, while the untreated rGO sensor showed an increase of only 3.53%. In addition, **Fig. S2** shows the changes in the resistance of the sensors, $(R_{ab}-R)/R$, caused by the immobilization of the antibody on the rGO surfaces. These results indicated that antibody immobilization was affected by the conditions used for the oxygen plasma treatment. The resistance of the untreated rGO sensor and those of the rGO sensors treated with an oxygen plasma under mild conditions (i.e., at 25 W for 10, 20, 30 s) increased by 3.53%, 3.56%, 4.02% and 4.66%, respectively, after antibody immobilization. Further, the rGO sensors plasma treated at RF powers of 50 W and 100 W for 10 and 30 s exhibited increases in resistances of 13.9 and 22.9%. These results implied that while mild oxygen plasma treatment conditions reliably preserved the rGO films, they did not significantly

functionalize the surfaces of the films when compared to that of the untreated rGO sample. Given that the loss in the inherent characteristics was minimal and the enhancement in the surface functionality with respect to biomolecules was of the desirable level, the optimal conditions for the oxygen plasma treatment were determined to be an RF power of 50 W and an exposure time of 10 s.

The results of the topographic analyses of the untreated and oxygen-plasma-treated rGO surfaces can be seen in the inset images in **Fig. 4A**. The surface topologies of various nanobiomaterials and molecules on diverse substrates have been analyzed previously using AFM (H. Lee et al., 2016). Based on the results of previous studies, the measured size of the antibody molecules was assumed to be 7–9 nm, as determined using an image-processing software, Image Pro Plus (Media Cybernetics, Inc., Silver Spring. MD). This allowed for a quantitative examination of the functionalized antibody molecules on the rGO surfaces subjected to the oxygen treatment under different conditions. The untreated (N = 16, **Fig. 4A**, left inset) and oxygen-plasma-treated rGO surfaces (N = 16, **Fig. 4A**, right inset) were analyzed, and the numbers of antibody molecules were determined to be 119 ± 20.25 and 218 ± 26.1 per unit area, respectively, over an area of 5 μm × 5 μm. The wrinkles on the surfaces of the rGO films were deliberately excluded from the analysis. The results of these surface density measurements of the antibody molecules confirmed that the functionality of rGO was enhanced after the oxygen plasma treatment.

Next, $A\beta_{1\text{-}42}$ peptides (Sigma Aldrich, USA) were diluted in a 10 mM PBS solution and introduced on the untreated and oxygen-plasma-treated rGO sensors to test for target-specific recognition by the functionalized antibody; the negative control was also tested similarly. **Fig. 4B** shows a plot of the change in resistance, $(R_{rec}\text{-}R_{ab})/R_{ab}$, as a function of the concentration of the target analytes on a logarithmic scale; here, R_{rec} is the resistance measured immediately

after the target-specific recognition of the peptides on the antibody-functionalized rGO surfaces. The changes in the resistance of both the untreated and the oxygen-plasma-treated rGO sensors exhibited a linear relationship with the analyte concentration from 100 fg mL^{-1} to 1 ng mL^{-1}. Compared to the slope of the curve in the case of the untreated rGO sensor, that of the curve for the oxygen-plasma-treated rGO sensors was 3.33 steeper.

Further, the PSA antibody (10 μg mL^{-1}, Covance, USA) which exhibits non-binding specificity to target analytes, was immobilized on the oxygen-plasma-treated rGO surfaces as a negative control. Then, the $A\beta_{1-42}$ peptides were introduced on the sensors in a similar concentration. On estimating the slope of the curve corresponding to the nonspecific binding interactions, no significant interaction between the nonspecific antibody and the target analytes was observed in the case of the oxygen-plasma-treated rGO sensors. These results confirmed that the oxygen plasma treatment increased the reactivity and hence the degree of functionalization of the rGO surfaces, allowing for enhanced interactions between the functionalized antibody molecules and the target analytes.

3.3 The aging behavior of oxygen-plasma-treated rGO sensors

It is well known that a plasma treatment of a material increases its wettability and results in functional groups being bonded to its surface. However, surface modifications performed through plasma treatments are not permanent and the effects of the modification gradually weaken with time; this phenomenon is defined as aging (Everaert et al., 1995; Gerenser et al., 1985; Yun et al., 2004). It has been suggested that the diffusion and reaction of free radicals or the reorientation of polar surface groups results in the thermodynamically favorable orientation of functional groups on the surfaces of plasma-treated materials (Bodas et al., 2008; Murakami et al., 1998). To confirm these time-dependent recovery characteristics from

the perspective of the biological reactivity of the modified surfaces, we monitored the changes in the resistance of the plasma-treated rGO surfaces subjected to antibody immobilization and target-specific recognition interactions after they had been aged for different durations in dry air. The rGO sensors were stored and exposed to air at room temperature immediately after the oxygen plasma treatment for 0, 3, 6, 9, and 24 h. **Fig. 5A** shows that the biological reactivity with respect to antibody immobilization and target-specific recognition diminished with an increase in the aging time. The resistance after antibody immobilization decreased drastically by 44% after aging for 6 h but remained constant thereafter. In addition, the resistance after target-specific recognition interactions with the Aβ peptides also decreased by 51% after aging by 6 h. In order to support the studies of the enriched functionality on rGO surfaces and the time-dependent behavior of oxygen plasma treatment on rGO surfaces, the rGO surfaces were pretreated with 5 M ETA in order to chemically block their active sites before antibody immobilization. ETA is commonly used as a blocking agent after protein coupling by covalent bonding with remaining reactive functional groups (Balcer et al., 2003; Frederix et al., 2004). The changes in the resistance, $(R_{ETA}-R)/R$, of the rGO sensors subjected to the ETA pretreatment are shown in **Fig. 5B**; here, R_{ETA} is the resistance of the rGO sensors after the ETA treatment and R is the initial resistance of the sensors before functionalization. The oxygen-plasma-treated rGO sensors showed a response 1.68-fold higher than that of untreated rGO. The changes in the resistance, $(R_{ab}-R_{ETA})/R_{ETA}$), of the untreated and oxygen-plasma-treated rGO sensors after sequential antibody immobilization were 2.59% and 7.17%, respectively (**Fig. 5C**). **Fig. S3A** shows the surface topologies of the ETA-pretreated rGO surfaces after antibody immobilization. The particles with the particular size were counted as 61 ± 19.76 ea in a limited area of 5 μm × 5 μm (N = 16). In comparison with the results with the untreated and oxygen-plasma-treated rGO sensors, the number of counted particles summarized in **Fig. S3B** and the tendency was

clearly seen among different conditions of rGO surfaces. These results indicated that, when the rGO surfaces were pretreated with the blocking agent (ETA) in a high concentration, the ETA molecules occupied the active sites on the rGO surfaces, thus hindering the sequential immobilization of the antibody molecules. Thus, the changes in the resistances of both the untreated and the plasma-treated rGO sensors in response to antibody immobilization were lower after the ETA pretreatment. Next, the effects of the ETA pretreatment and subsequent antibody immobilization on the plasma-treated rGO surfaces aged for different durations were also investigated. **Fig. S4** shows that the change in the resistance, $(R_{ETA}-R)/R$, after the ETA blocking treatment decreased gradually from 24.7% to 15.2% after aging for 24 h while that after antibody immobilization decreased significantly by 35.8% after aging for 6 h. **Fig. 5D** shows a comparison of the extent of antibody immobilization on the plasma-treated rGO surfaces whether oxygen plasma treatment with the blocking agent with aging.

These results confirmed the following two facts: the binding functionality of the rGO surfaces, resulting from covalent bonding, was improved by the oxygen plasma treatment, and the enhancement in the reactivity decreased with aging in dry air at room temperature. The plasma-treated rGO sensors formed a greater number of covalent bonds with the antibody molecules. Consequently, they exhibited enhanced sensing performance with respect to the target analytes as compared to the untreated rGO sensor. This strategy of surface modification by packing an antibody on the reactive surfaces increased their sensitivity with respect to the detection of the target analytes. Meanwhile, several studies have used contact-angle measurements and chemical analysis to show that the surface energy of oxygen-plasma-treated materials exhibits time-dependent recovery behavior. Morra et al. (Morra et al., 1990) reported that the hydrophobicity of an oxygen-plasma-treated polydimethylsiloxane surface returned after aging for different durations at different temperatures. They monitored the change in the hydrophobicity at room temperature over a

period of 6–19 h. In addition, a previous study in which epitaxial graphene was subjected to an oxygen plasma treatment under mild conditions also found that the characteristics of the plasma-treated sample returned to their initial state within 24 h (Shin et al., 2010). In this regard, the fact that that the biological reactivity of the plasma-treated rGO sensors returned to its initial state after 6–9 h was within expectations and suggested that the plasma-treated rGO sensors should be used immediately after the plasma treatment, in order to ensure that they exhibit enhanced sensing performance.

3.4 Test of sensor with human-derived exosomal samples for clinical application

To determine the feasibility of using the oxygen-plasma-treated rGO sensors for clinical diagnosis, we extracted neural-derived exosomal Aβ peptides from the AD and NC samples and used the sensors for distinguishing the peptides. As shown in **Fig. 6a**, the neural-derived exosomes were isolated from human plasma using ExoQuick-based precipitation and centrifugation (Fiandaca et al., 2015; Mitsuhashi et al., 2013). The extracted exosomes were lysed with an radioimmunoprecipitation assay buffer to release the Aβ peptides from the inner membrane. Generally, plasma samples from AD patients contain larger quantities of Aβ peptides and their aggregates than do those from NC subjects (Villemagne et al., 2013). The prepared exosomal Aβ peptides were incubated with the rGO sensors for 30 m to ensure specific binding interactions with the antibody molecules on the rGO surfaces.

When identical AD and NC samples were introduced on the untreated and plasma-treated rGO sensors, the changes in the resistance of the plasma-treated rGO sensors in response to the AD and NC samples were 4.28% and 1.55%, respectively; in comparison, the untreated rGO sensor showed resistance changes of 2.14% and 1.70% in the case of the AD and NC samples, respectively (**Fig. 6B**). The changes in the resistance in response to the AD and NC samples in the case of the oxygen-plasma-treated rGO sensors were significantly different (p

< 0.001), in contrast to the case for the untreated rGO sensors (p = 0.0460). This result indicated that the oxygen-plasma-treated rGO sensors exhibited good performance in the clinical identification of AD and NC subjects based on the detection of target analytes.

Finally, a number of AD (N = 15) and NC samples (N = 15) were introduced on the oxygen-plasma-treated rGO sensors, in order to confirm the determination of the status of patients. **Fig. 6C** shows the cross-sectional comparisons of the statistical analysis. The changes in the resistance, $(R_{rec}-R_{ab})/R_{ab}$, resulting from the interaction with the exosomal Aβ peptides derived from the AD subjects were distributed and depended on the samples; however, the changes were greater (1.75–7.09%) than those in the case of the NC samples (0.02–1.79%). We could also confirm the selectivity of the rGO sensors in a negatively controlled environment by immobilizing a PSA antibody instead of the 6E10 antibody. The resistance changed by only 1.69% in the case of the negatively controlled rGO sensors. The results obtained in the case of the NC samples and the negative control might be attributable to the nonspecific binding or undesirable adsorption of the biomolecules in question.

4. Conclusion

Oxygen plasma treatment is a simple and efficient approach for enhancing the biological reactivity of rGO surfaces. In this study, the optimal conditions for subjecting rGO surfaces to an oxygen plasma treatment without causing a loss in the inherent properties of the prepared rGO films were determined. Based on the changes in the resistance caused by antibody immobilization and the target-specific recognition of Aβ peptides, it was confirmed that plasma treatment increased the sensitivity of the rGO surfaces with respect to biological interactions. The electrical response of the rGO sensors after antibody immobilization and the slope of the curve representing the target-specific interactions of the rGO surfaces were enhanced by 3.94 and 3.33 times, respectively. Further, the effects of the oxygen plasma

treatment were found to be time dependent. In addition, the rGO surfaces were pretreated with a blocking agent on the functional groups, in order to elucidate the phenomenon. The obtained results implied that the increment in the biological functionality was time dependent, as is the case for the surface modification resulting from an oxygen plasma treatment. Finally, samples taken from AD and NC subjects could be identified successfully using the oxygen-plasma-treated rGO sensors as a diagnostic tool for statistical analysis. These results suggested that using an oxygen plasma treatment for modifying the rGO surfaces enhanced their biomolecule-sensing performance without requiring additional complex procedures such as nanoparticle-conjugated labeling and that this surface-modification method should aid in the development of novel diagnostic tools based on carbon nanomaterials.

Appendix A. Supplementary material

Notes

The authors declare no competing financial interest.

Acknowledgements

The authors are grateful for financial support from the Korea Institute of Science and Technology (KIST) Institutional Program (2V04870 & 2E26180) and the Korea Health Industry Development Institute (KHIDI) (HI14C3319).

References

Balasubramanian, K., Kern, K., 2014. Adv. Mater. 26, 1154–1175.

Balazs, D.J., Triandafillu, K., Chevolot, Y., Aronsson, B.O., Harms, H., Descouts, P., Mathieu, H.J., 2003. Surf. Interface Anal. 35, 301–309.

Balcer, H.I., Spiker, J.O., Kang, K.A., 2003. Adv. Exp. Med. Biol. 530, 133–141.

Beams, R., Gustavo Cançado, L., Novotny, L., 2015. J. Phys.-Condes. Matter 27, 083002.

Bodas, D., Rauch, J.-Y., Khan-Malek, C., 2008. Eur. Polym. J. 44, 2130–2139.

Childres, I., Jauregui, L.A., Tian, J., Chen, Y.P., 2011. New J. Phys. 13.

Chirila, V., Marginean, G., Brandl, W., 2005. Surf. Coat. Technol. 200, 548–551.

Everaert, E.P., Van Der Mei, H.C., Vries, J.D., Busscher, H.J., 1995. J. Adhes. Sci. Technol. 9, 1263–1278.

Fiandaca, M.S., Kapogiannis, D., Mapstone, M., Boxer, A., Eitan, E., Schwartz, J.B., Abner, E.L., Petersen, R.C., Federoff, H.J., Miller, B.L., Goetzl, E.J., 2015. Alzheimers. Dement. 11, 600–607.

Frederix, F., Bonroy, K., Reekmans, G., Laureyn, W., 2004. J. Biochem. Biophys. Methods 58, 67–74.

Gerenser, L.J., Elman, J.F., Mason, M.G., Pochan, J.M., 1985. Polymer 26, 1162–1166.

Hernández, R., Vallés, C., Benito, A.M., Maser, W.K., Rius, F.X., Riu, J., 2014. Biosens. Bioelectron. 54, 553–557.

Huang, X., Yuan, T., Tschannen, M., Sun, Z., Jacob, H., Du, M., Liang, M., Dittmar, R.L., Liu, Y., Liang, M., Kohli, M., Thibodeau, S.N., Boardman, L., Wang, L., 2013. BMC Genomics 14, 319.

Jang, H.D., Kim, S.K., Chang, H., Choi, J.-W., 2015. Biosens. Bioelectron. 63, 546–551.

Kim, D.-J., Yung Sohn, Il, Jung, J.-H., Yoon, O.J., Lee, N.E., Park, J.-S., 2013. Biosens. Bioelectron. 41, 621–626.

Kim, J., Chae, M.-S., Lee, S.M., Jeong, D., Lee, B.C., Lee, J.H., Kim, Y., Chang, S.T., Hwang, K.S., 2016. Sci. Rep. 6, 31276.

Kim, N.H., Kim, B.J., Ko, Y., Cho, J.H., Chang, S.T., 2012. Adv. Mater. 25, 894–898.

Kim, Y.-K., Kim, M.-H., Min, D.-H., 2011. Chem. Commun. 47, 3195–3.

Ko, Y., Kim, N.H., Lee, N.R., Chang, S.T., 2014. Carbon 77, 964–972.

Kochmann, S., Hirsch, T., Wolfbeis, O.S., 2012. Trac-Trends Anal. Chem. 39, 87–113.

Lee, H., Lee, W., Lee, J.H., Yoon, D.S., 2016. J. Nanomater. 2016, 1–21.

Lee, J.-Y., Park, E.-J., Lee, C.-J., Kim, S.-W., Pak, J.J., Min, N.K., 2009. Thin Solid Films 517, 3883–3887.

Lu, C.H.H., Yang, H.H.H., Zhu, C.H.L., Chen, X., Chen, G.H.N., 2009. Angew. Chem. 121, 4879–4881.

Mao, H., Di Wu, Wu, W., Xu, J., Hao, Y., 2009. Nanotechnology 20, 445304.

McKhann, G., Drachman, D., Folstein, M., Katzman, R., 1984. Neurology 34, 939–939.

Mitsuhashi, M., Taub, D.D., Kapogiannis, D., Eitan, E., Zukley, L., Mattson, M.P., Ferrucci, L., Schwartz, J.B., Goetzl, E.J., 2013. FASEB J. 27, 5141–5150.

Morra, M., Occhiello, E., Marola, R., Garbassi, F., Humphrey, P., Johnson, D., 1990. J. Colloid Interface Sci. 137, 11–24.

Murakami, T., Kuroda, S.I., Osawa, Z., 1998. J. Colloid Interface Sci. 202, 37–44.

Murphy, M.P., LeVine, H., III, 2010. J. Alzheimers. Dis. 19, 311–323.

Nourbakhsh, A., Cantoro, M., Vosch, T., Pourtois, G., Clemente, F., van der Veen, M.H., Hofkens, J., Heyns, M.M., De Gendt, S., Sels, B.F., 2010. Nanotechnology 21, 435203

O'Brien, R.J., Wong, P.C., 2011. Annu. Rev. Neurosci. 34, 185–204.

Ohno, Y., Maehashi, K., Matsumoto, K., 2010. J. Am. Chem. Soc. 132, 18012–18013.

Peterson, M.F., Otoc, N., Sethi, J.K., Gupta, A., Antes, T.J., 2015. Methods 87, 1–15.

Roh, J.H., Qiu, A., Seo, S.W., Soon, H.W., Kim, J.H., Kim, G.H., Kim, M.-J., Lee, J.-M., Na, D.L., 2011. J. Neurol. 258, 1013–1020.

Schedin, F., Geim, A.K., Morozov, S.V., Hill, E.W., Blake, P., Katsnelson, M.I., Novoselov, K.S., 2007. Nat. Mater. 6, 652–655.

Shin, Y.J., Wang, Y., Huang, H., Kalon, G., Wee, A.T.S., Shen, Z., Bhatia, C.S., Yang, H., 2010. Langmuir 26, 3798–3802.

Villemagne, V.L., Burnham, S., Bourgeat, P., Brown, B., 2013. Lancet Neurol. 12, 357–367

Xue, C.-Y., Yang, K.-L., 2007. Langmuir 23, 5831–5835.

Yun, Y.I., Kim, K.S., Uhm, S.-J., Khatua, B.B., Cho, K., Kim, J.K., Park, C.E., 2004. J. Adhes. Sci. Technol. 18, 1279–1291.

FIGURE LEGENDS

Fig. 1. Schematic representation of the enhancement of biological reactivity on rGO surface with oxygen plasma treatment for antibody immobilization and specific recognition between the target and antibody. The rGO sensor relying on relative changes of electric resistance allow detection of molecular interactions on the surfaces.

Fig. 2. (A)−(D) schematic illustration of fabrication process (A) deposition of rGO thin film on Si/SiO_2 substrate by using the MDD method. (B) rGO patterning with photolithography (C) Au pads formation by lift-off technique (D) additional oxygen plasma treatment on rGO surfaces. (E) Photographs of a fabricated rGO sensor including 14 arrays of rGO patterns and (F) an optical image of a rGO pattern. (the scale bar is 100 μm.)

Fig. 3. (A) The effect of oxygen plasma treatment with different exposure conditions of (A) a thickness profile (black symbol and line) and (B) resistance changes $(R_{oxy}\text{-}R)/R_0$ compared to initial values (R_0) (red block).

Fig. 4. Comparison of biological reactivity between the untreated and plasma treated rGO surfaces by measuring (A) resistance change $(R_{ab}\text{-}R)/R$ before and after immobilization of monoclonal 6E10 antibody on the surfaces and topographic analysis for counting the number of immobilized antibodies with a particular size (7~ 9nm). The inset AFM images (5×5 μm^2) with antibody-immobilized surface of the (left) untreated and (right) oxygen-plasma-treated rGO sensors (The scale bar is 1 μm.) (B) Responses of resistance changes versus concentration of $A\beta_{42}$ peptides on the logarithmic scale; target-specific antibody oxygen-plasma-treated (red symbols) and untreated (blue symbols) rGO sensors and for negatively controlled rGO sensors (black symbols). The calibration lines are fitted by linear relation between resistance changes $(R_{rec}\text{-}R_{ab})/R_{ab}$ and logarithmic concentration.

Fig. 5. Comparison of biological reactivity between the untreated and plasma treated rGO surfaces by measuring (A) resistance change $(R_{ab}-R)/R$ before and after immobilization of monoclonal 6E10 antibody on the surfaces and (B) $(R_{rec}-R_{ab})/R_{ab}$ of target-specific recognition of 100 pg mL^{-1} Aβ peptides. (C) The resistance changes of antibody immobilization and sequential target-specific recognition via plasma treated rGO sensor with different aging time.

Fig. 6. (A) schematic diagram of sample preparations for neural-derived exosomal Aβ peptides and molecular interactions on surface of rGO sensor. (B) enhancement of sensing performance for discrimination of neural-derived exosomal Aβ peptides of human samples of AD and NC with comparison between untreated and plasma treated rGO sensors. (C) Comparison of ΔR/R responses by target-specific recognition with Aβ peptides in neural-derived exosomes isolated by human samples of AD (N = 15) and NC (N = 15) and negative control with 10 mM PBS buffer solution only. (* significant at $p < 0.05$, *** significant at $p < 0.001$)

Highlights

> Oxygen plasma treatment improved the biological functionality of reduced graphene oxide (rGO) biosensors.
> The effects of oxygen plasma treatment on rGO biosensors were investigated.
> Oxygen-plasma-treated rGO biosensors showed 3.33-fold greater responses in target specific recognition.
> Identification of Alzheimer's disease patients and normal control was performed by use of exosomal samples.
> The oxygen-plasma-treated rGO biosensors showed the feasibility of a diagnostic tool for Alzheimer's Disease.

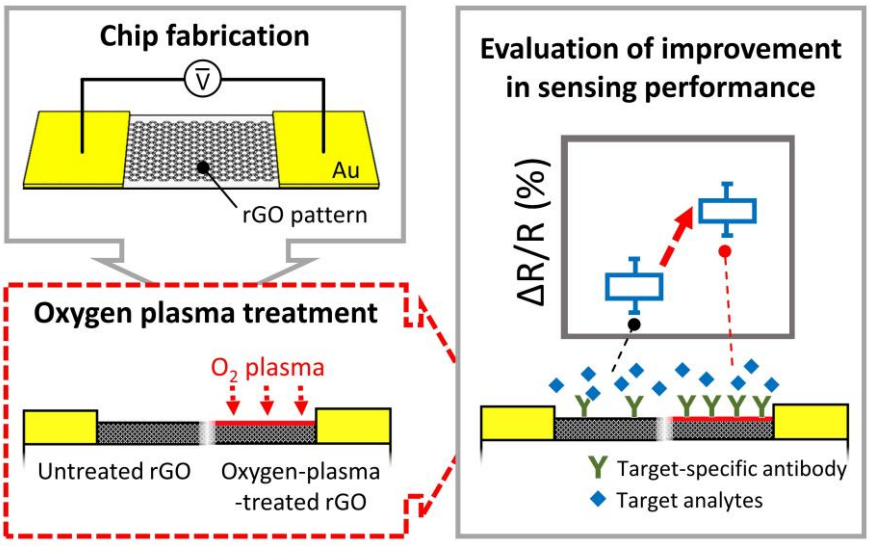

Fig. 1

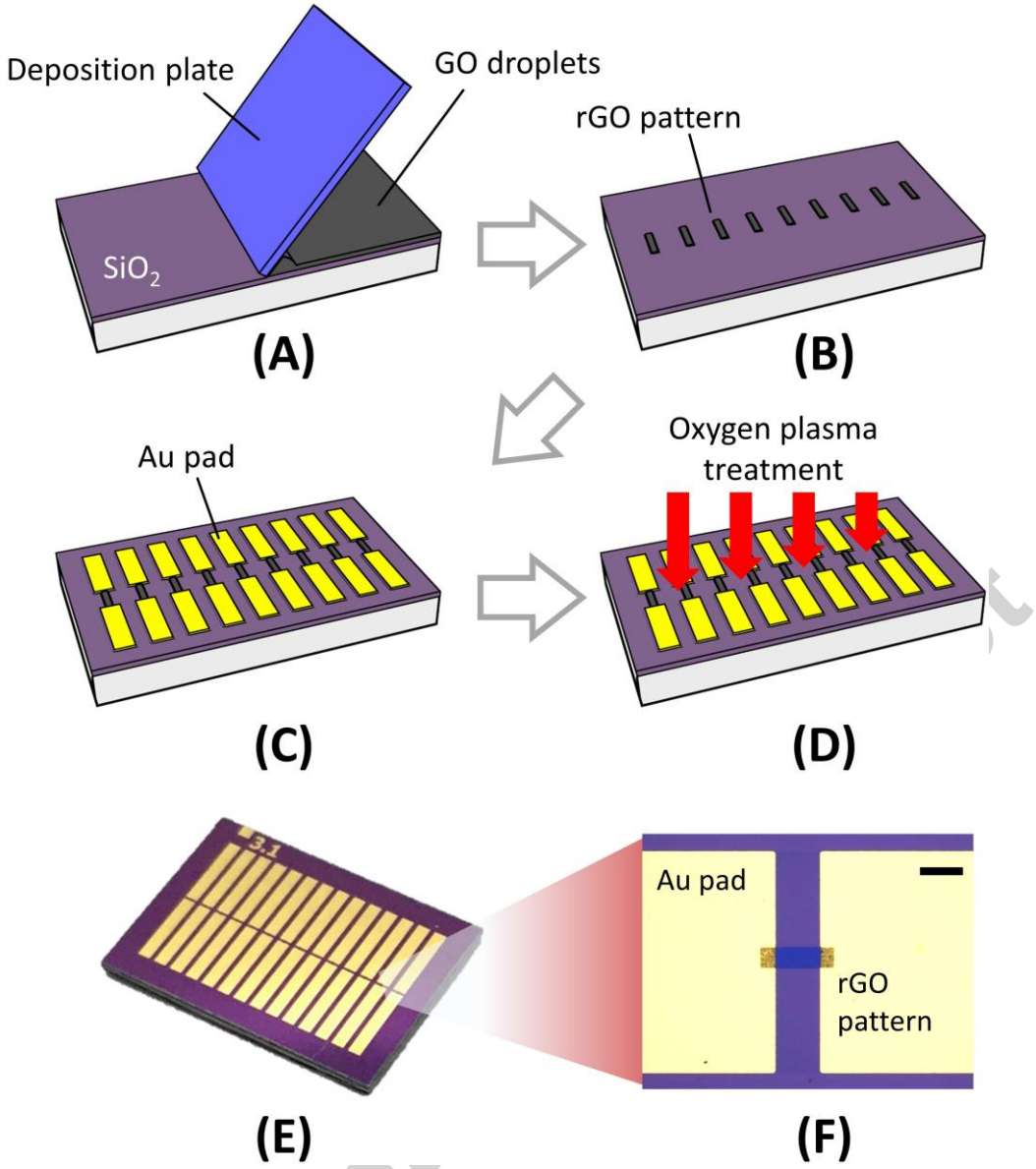
Deposition plate
GO droplets
SiO_2
(A)
rGO pattern
(B)
Au pad
Oxygen plasma
treatment
(C)
(D)
Au pad
rGO
pattern
(E)
(F)

fig. 2

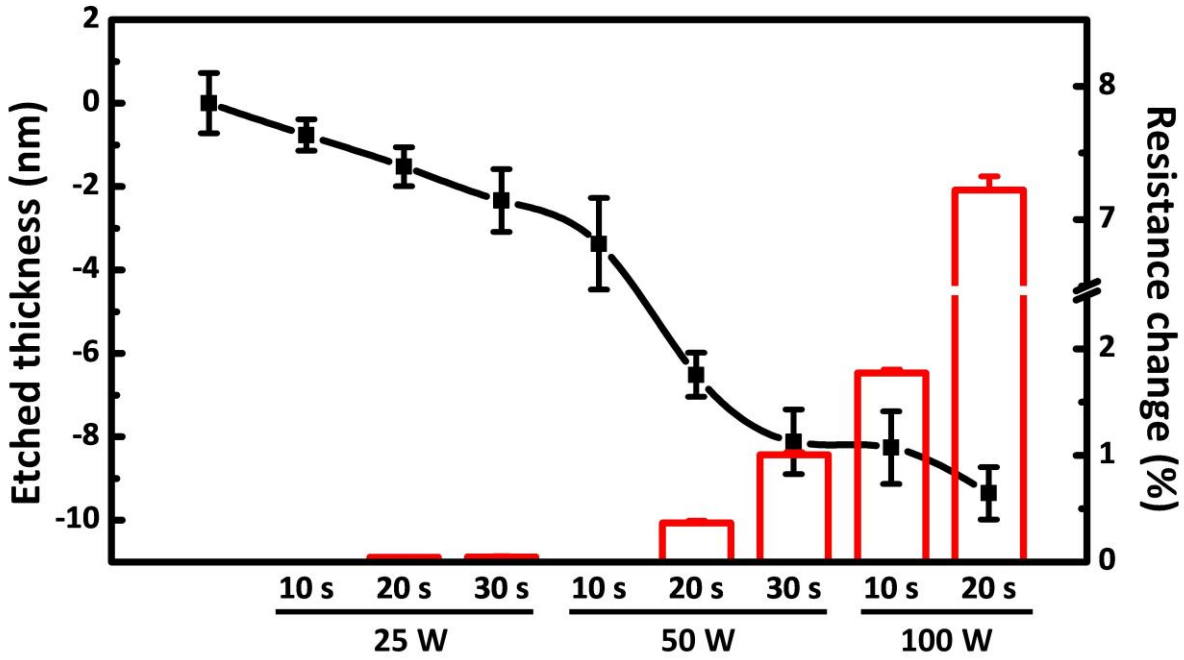

fig 3

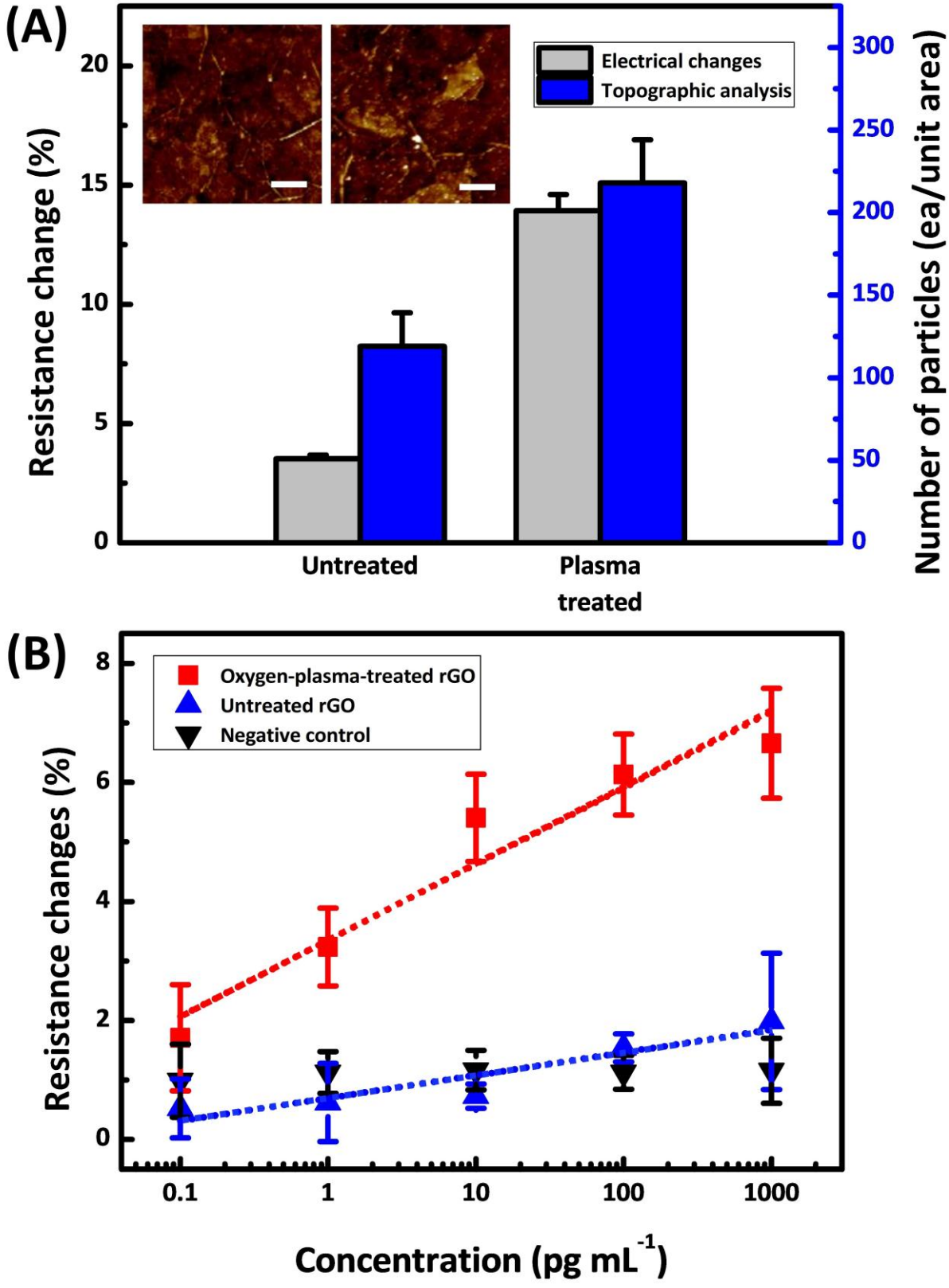
(A)
Resistance change (%)
Number of particles (ea/unit area)
Electrical changes
Topographic analysis
Untreated
Plasma treated
(B)
Oxygen-plasma-treated rGO
Untreated rGO
Negative control
Resistance changes (%)
Concentration (pg mL-1)

fig 4

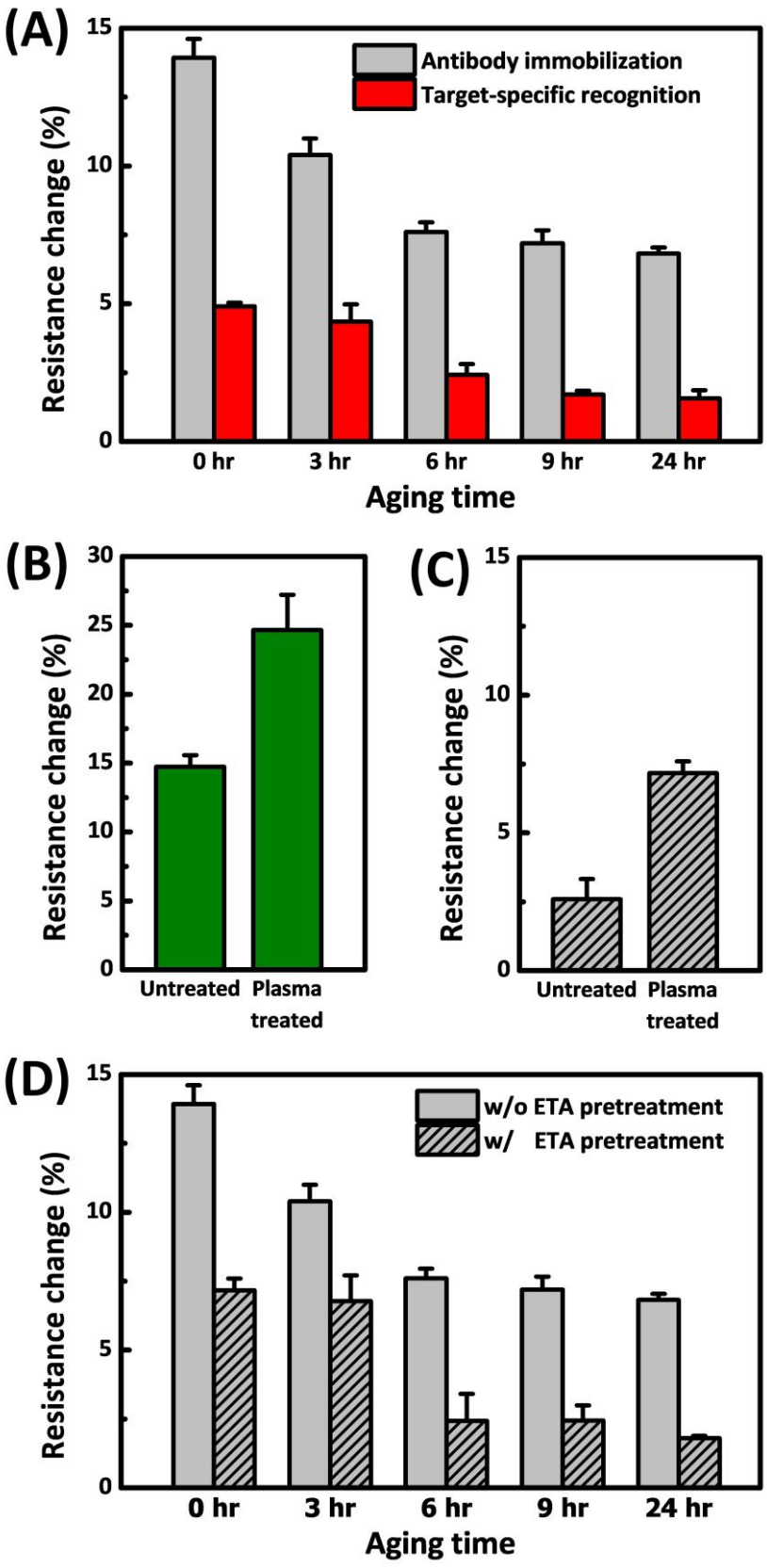
(A)
Antibody immobilization
Target-specific recognition
Resistance change (%)
0
5
10
15
0 hr
3 hr
6 hr
9 hr
24 hr
Aging time
(B)
Resistance change (%)
0
5
10
15
20
25
30
Untreated
Plasma treated
(C)
Resistance change (%)
0
5
10
15
Untreated
Plasma treated
(D)
w/o ETA pretreatment
w/ ETA pretreatment
Resistance change (%)
0
5
10
15
0 hr
3 hr
6 hr
9 hr
24 hr
Aging time

fig 5

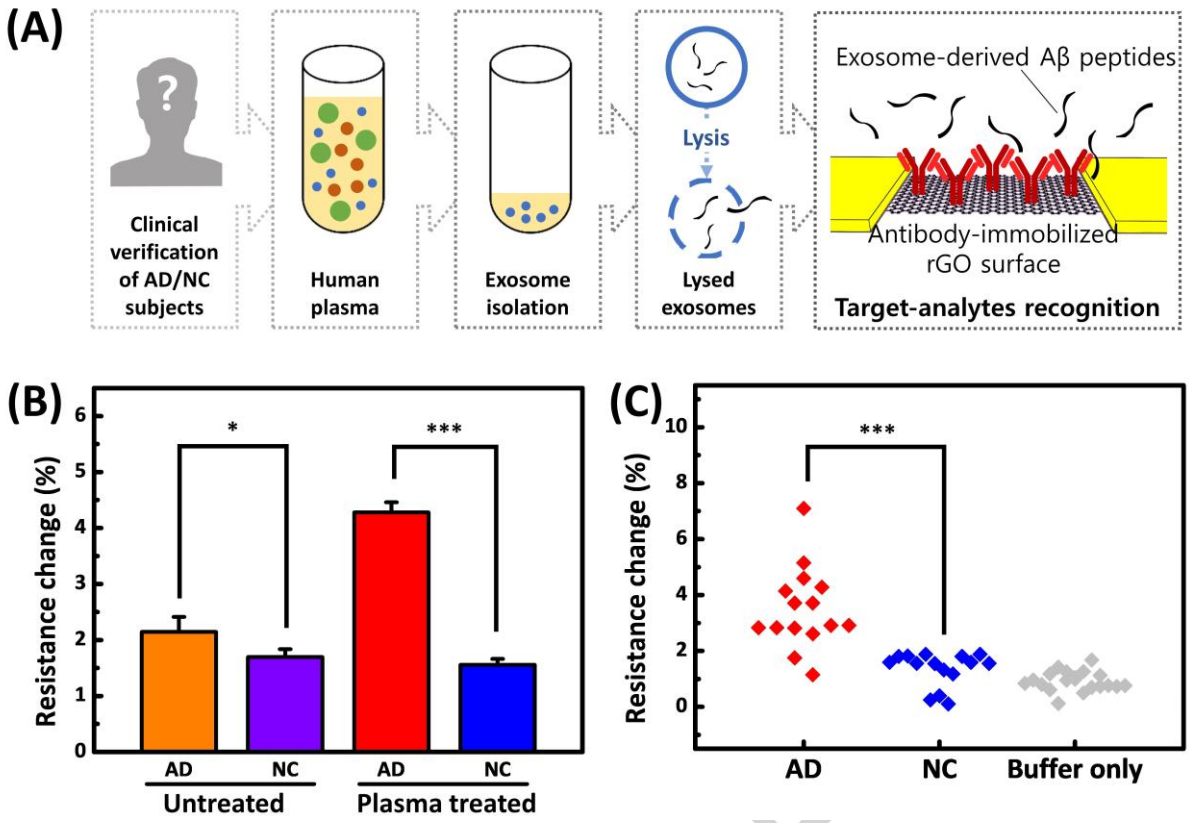

fig 6